

ClinKD: Cross-Modal Clinic Knowledge Distiller For Multi-Task Medical Images

Hongyu Ge¹, Longkun Hao^{1*}, Zihui Xu^{1*}, Zhenxin Lin², Bin Li^{3†}, Shoujun Zhou^{3†},
Hongjin Zhao⁴, Yihang Liu¹

¹ Shandong University

² Hubei University

³ Shenzhen Institutes of Advanced Technology, Chinese Academy of Sciences

⁴ Australian National University

Abstract

Med-VQA (Medical Visual Question Answering) is a crucial subtask within the broader VQA (Visual Question Answering) domain. This task requires a visual question answering system to analyze the provided image and corresponding question, offering reasonable analysis and suggestions to assist medical professionals in making pathological diagnoses, or ideally, enabling the system to independently provide correct diagnoses. Furthermore, more advanced Med-VQA tasks involve Referring and Grounding, which not only require the system to accurately comprehend medical images but also to pinpoint specific biological locations within those images. While many large pre-trained models have demonstrated substantial VQA capabilities, challenges persist in the medical imaging domain. The intricacy of biological features in medical images and the scarcity of high-quality medical image datasets, combined with the fact that current models are not tailored for the medical field in terms of architecture and training paradigms, hinder the full exploitation of model generalization. This results in issues such as hallucination in Visual Grounding. In this paper, we introduce the ClinKD model, which incorporates modifications to model position encoding and a diversified training process. Initially, we enhance the model’s ability to perceive image and modality variations by using Med-CLIP Guided Rotary Position Embedding. Subsequently, we leverage distillation to provide prior knowledge to the model before using complete training data. Additionally, the feedback-based training process during the formal training phase further enhances data utilization. Notably, under unchanged evaluation protocols, we achieve a new state-of-the-art performance on the Med-GRIT-270k dataset, and the Med-CLIP Guided Rotary Position Embedding approach presents potential for generalizing to universal model position encoding.

Introduction

Medical Visual Question Answering (Med-VQA) is a critical domain for applying large language model (LLM) technologies to medical analysis. With the continuous evolution of multimodal large model architectures and training paradigms, Med-VQA has achieved preliminary capabilities in image analysis, annotation, and user instruction compli-

ance. Previous studies have made multiple attempts to enhance the generalization performance of multimodal models on medical data. For instance, LLaVA-Med (Li et al. 2023), the first medical assistant that extends instruction-tuning techniques for multimodal models to the medical domain. This work leveraged instruction tuning and curated image-text datasets to align visual-textual features in LLaVA (Liu et al. 2023), enabling it to recognize and analyze medical images. However, this system lacked fine-grained image understanding, failing to precisely localize anatomically specified regions in instructions. Subsequently, the BiRD (Huang et al. 2024), a model which incorporated fine-grained image recognition by developing a Biomedical Refer-and-Ground Instruction-Tuning Dataset. This led to the first Biomedical Refer-and-Ground Multimodal Large Language Model, addressing the absence of grounding capabilities in LLaVA. Nevertheless, due to its reliance on traditional supervised learning and conventional 2D rotary positional encoding, BiRD struggled to capture cross-axis dependencies in medical imaging (e.g., MRI/CT) or generalize to unseen medical domains, resulting in subpar performance on Visual Grounding (VG) tasks (e.g., poor MR-based VG evaluation results as noted in the original paper).

Current research still overlooks the unique challenges of medical image feature extraction. Unlike natural images, most medical features manifest as grayscale variations rather than color differences, and fine-grained positional dependencies across height and width dimensions require greater emphasis. Thus, models must be enhanced to improve cross-axis recognition capabilities. Additionally, optimizing model performance under limited data remains a significant challenge.

To overcome these limitations, we propose a medical distillation framework (ClinKD) to boost VQA capabilities. Specifically: 1. Model Architecture: We integrate Med-CLIP-Guided Rotary Position Embedding to enhance cross-axis perception across image height and width dimensions, addressing fine-grained feature extraction. 2. Training Strategy: We employ Pseudo-Augmented Medical Distillation with reflective correction. Untrained models generate pseudo-labels for distillation, providing prior knowledge before exposure to real medical data. During training, the model undergoes dual distillation using both self-generated

*These authors contributed equally.

†Corresponding Authors, Emails: {b.li2, sj.zhou}@siat.ac.cn

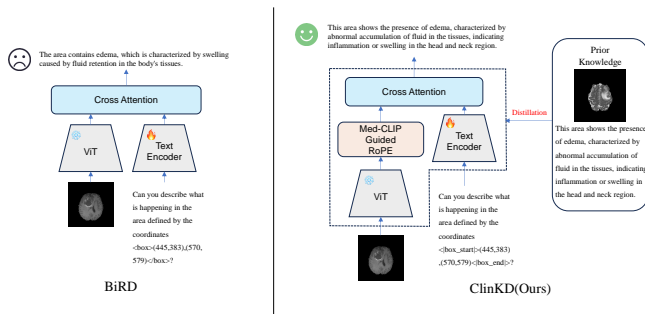


Figure 1: Why we need to do distillation

data (with error correction) and ground-truth labels, ensuring robustness against noisy pseudo-labels and improving generalization. 3. Inference Optimization: To prioritize diagnostic reliability, we adopt Semantic-Aware Selective Generation (SASG), which evaluates candidate responses based on confidence metrics to ensure high-quality, clinically interpretable outputs. Our contributions are summarized as follows:

- We integrate Med-CLIP-Guided Rotary Position Embedding into positional encoding, enabling better cross-dimensional feature capture in medical imaging.
- We propose ClinKD, a novel distillation framework combining Pseudo-Augmented Medical Distillation and Reflective Correction Training to mitigate prior knowledge gaps and enhance multitask generalization under data scarcity.
- We design SASG, a confidence-driven response selection strategy, to reduce output randomness and improve diagnostic coherence.
- ClinKD achieves state-of-the-art performance on the Med-GRIT-270k dataset, particularly excelling in VG tasks.

Related Work

Multimodal Large Language Models For Biomedicine(MLLMs) With the development of multimodal large language models, an increasing number of approaches have been applied to the medical field, such as BioMedGPT, LLaVa-Med, and BiRD. These methods drive the development of multimodal models in the biomedical domain from different perspectives. For instance, LLaVA-Med researchers were the first to apply instruction fine-tuning techniques to the medical imaging field and built a medical question-answering system based on LLaVA, which provides reasonable responses by processing user-submitted images and instructions. However, LLaVA-Med does not support fine-grained interactions with images, meaning that the system cannot precisely locate specific regions within the images. To address this lack of referring and grounding capabilities, Xiaoshuang Huang and colleagues proposed BiRD, and their Med-GRIT-270k (Huang et al. 2024) dataset includes multitask data that, under instruction fine-tuning, equips Qwen-VL with referring and

grounding capabilities. However, BiRD does not consider the model’s ability to capture medical image features at the model level, and the training details follow the traditional instruction fine-tuning approach, which cannot address the issue of the vision encoder being exposed to insufficient medical data before being frozen during pretraining. No solution has yet emerged to fully address these challenges.

Chain of Thought Chain of Thought (CoT) (Wei et al. 2023) is a prompting technique designed to assist language models in complex reasoning and cognitive processes. It guides the model to solve problems step by step, presenting a series of coherent steps that illustrate the reasoning and logical relationships. Research on multimodal CoT, such as DD-CoT (Zheng et al. 2023), incorporates multimodal elements into the reasoning process by dividing the target into subproblems. Analyzing these subproblems enhances the accuracy of the main problem’s response and mitigates the hallucination issue in multimodal models. In the field of medical VQA, the introduced Med-CoT (Liu et al. 2024), which combines the effects of Chain of Thought and MoE (Mixture of Experts) is used to distinguish between effective and ineffective answers, ultimately selecting the final answer through the MoE model. This expert model, which decomposes problems using the Chain of Thought, demonstrates strong generalization capabilities and interpretability. However, Med-CoT is still limited by the capabilities of both the base model and the expert model. The foundational abilities of the model’s vision encoder remain limited, making it susceptible to hallucinated answers. Currently, solutions addressing the hallucination problem in medical VQA are still scarce.

Knowledge Graph(KG) Knowledge graphs represent a set of relationships among entities. In the context of medical knowledge graphs, recent research such as ImgFact employs multimodal knowledge graphs through triplets, leveraging structured relationships for inference tasks. Generating Natural Language Explanations (NLEs) for medical images is similar to medical VQA in that it relies on the visual-language modality to answer questions concerning visual information. Ameer Hamza and colleagues proposed a KG-based RAG system (Hamza et al. 2024) that constructs a knowledge graph as a database for multimodal models, thereby simulating the way radiologists accumulate experience and knowledge. This approach enhances both the accuracy and information richness of the model’s generated responses, partially mitigating the hallucination problem. However, if new modalities are introduced into such knowledge-graph-based models, the corresponding graph processing modules must be reselected and retrained.

Methodology

Med-CLIP Guided Rotary Position Embedding

While Qwen-VL achieves state-of-the-art performance using absolute position embeddings, we argue that absolute positioning limits the model’s focus on the relative spatial relationships crucial for understanding medical data. In image-text joint training part, it is essential to account for

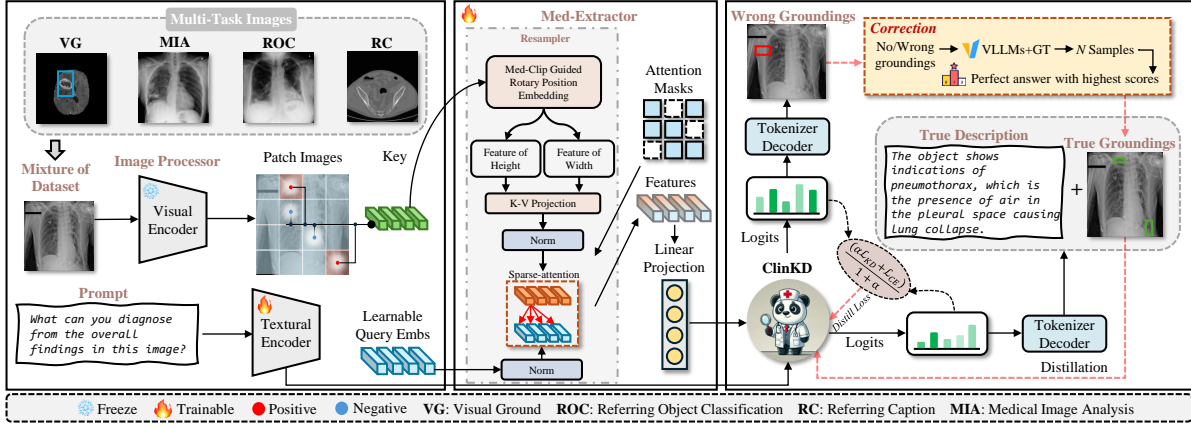


Figure 2: **Overview of our ClinKD’s framework:** The multi-task images will be patched by ViT and the key matrix will be processed by the Med-CLIP Guided RoPE which ensures features of height and width are extracted respectively. For training strategy, there are 2 steps. **Step 1:** Distilling the model by using pseudo labels. **Step 2:** Training (Distilling) the model by using whole dataset and the corrected data. The answer which has the highest scores among the N samples scored by CLIP models will be chosen as the final answer.

the modality-specific positional correlations between image patches and text tokens. To address this, we propose the Med-CLIP Guided Rotary Position Embedding (Med-CLIP Guided RoPE), which enhances the model’s ability to capture relative positional information that is highly relevant to medical content.

Suppose we have a Sentence-Image-Sentence position index sequence:

$$S_{idx} = (T_1, T_2, \dots, T_\ell, V_{\ell+1}, V_{\ell+2}, \dots, V_{\ell+wh}, T_{\ell+wh+1}, T_{\ell+wh+2}, \dots, T_{\ell+wh+k})$$

where $T_\ell = (t_\ell, t_\ell)$ is the end position index of the first sentence tokens, $V_i = (v_i^{(1)}, v_i^{(2)})$ is the image 2-dimension index.

Before we get RoPE of the sequence, we need to add scaling parameters and biases to the original images sequence position:

$$\mathcal{V}_i = (\alpha_1 v_i^{(1)} + \lambda_1, \alpha_2 v_i^{(2)} + \lambda_2)$$

In order to ensure the equivalence between the sentences before and after the image, the gap between the position of the last token of the first sentence and the first patch of the image should be equal to the gap between the last position of the image and the position of the first token of the second sentence. Therefore we get:

$$\begin{cases} \alpha_1 + \lambda_1 - \ell = \ell + wh + 1 - (\alpha_1 h + \lambda_1) \\ \alpha_2 + \lambda_2 - \ell = \ell + wh + 1 - (\alpha_2 w + \lambda_2) \end{cases}$$

We have 2 equations and 4 parameters: $\lambda_1, \lambda_2, \alpha_1, \alpha_2$. We need to fix α_1, α_2 first to set the gap between each image’s position index. So the general solution is

$$\begin{cases} \lambda_1 = \ell + \frac{wh+1-\alpha_1(h+1)}{2} \\ \lambda_2 = \ell + \frac{wh+1-\alpha_2(w+1)}{2} \end{cases}$$

where α_1, α_2 are hyperparameters. Hence we get position index of height:

$$S_{h-idx} = (t_1, \dots, t_\ell, \alpha_1 v_{\ell+1}^{(1)} + \lambda_1, \dots, \alpha_1 v_{\ell+wh}^{(1)} + \lambda_1, t_{\ell+wh+1}, \dots, t_{\ell+wh+k})$$

and position index of width:

$$S_{w-idx} = (t_1, \dots, t_\ell, \alpha_2 v_{\ell+1}^{(2)} + \lambda_2, \dots, \alpha_2 v_{\ell+wh}^{(2)} + \lambda_2, t_{\ell+wh+1}, \dots, t_{\ell+wh+k})$$

Suppose we have a query/key vector

$$q \in \mathbb{R}^{d_h+d_w}$$

we split it into two parts:

$$\begin{aligned} q^{(h)} &\in \mathbb{R}^{d_h} \\ q^{(w)} &\in \mathbb{R}^{d_w} \end{aligned}$$

And we set the frequency as below:

$$\begin{aligned} \omega_i^{(h)} &= 1/10000^{\frac{2i}{d_h}} \\ \omega_i^{(w)} &= 1/10000^{\frac{2i}{d_w}} \end{aligned}$$

If the height index of some token is h , then the angle of rotation will be:

$$\theta_i^{(h)} = h * \omega_i^{(h)}$$

while the width dimension case is calculated by the same procedure. Finally the Med-CLIP Guided RoPE on the height

dimension is given by:

$$\mathbf{R}_{\Theta,h}^{d_h} \mathbf{q}^{(h)} = \begin{pmatrix} q_1 \\ q_2 \\ q_3 \\ q_4 \\ \vdots \\ q_{d_h-1} \\ q_{d_h} \end{pmatrix} \otimes \begin{pmatrix} \cos \theta_1^{(h)} \\ \cos \theta_1^{(h)} \\ \cos \theta_2^{(h)} \\ \cos \theta_2^{(h)} \\ \vdots \\ \cos \theta_{d_h/2}^{(h)} \\ \cos \theta_{d_h/2}^{(h)} \end{pmatrix} + \begin{pmatrix} -q_2 \\ q_1 \\ -q_4 \\ q_3 \\ \vdots \\ -q_{d_h-1} \\ q_{d_h} \end{pmatrix} \otimes \begin{pmatrix} \sin \theta_1^{(h)} \\ \sin \theta_1^{(h)} \\ \sin \theta_2^{(h)} \\ \sin \theta_2^{(h)} \\ \vdots \\ \sin \theta_{d_h/2}^{(h)} \\ \sin \theta_{d_h/2}^{(h)} \end{pmatrix}$$

Where $\mathbf{R}_{\Theta,h}^{d_h}$ is the rotation matrix. The Med-CLIP Guided RoPE on width dimension can be calculated similarly. Finally, without losing the combination of the information of height and width dimension, we will put them together:

$$q_{RoPE} = \text{Concat}(\mathbf{R}_{\Theta,h}^{d_h} \mathbf{q}^{(h)} \mathbf{R}_{\Theta,w}^{d_w} \mathbf{q}^{(w)})$$

Pseudo-Augmented Medical Distillation

As the Qwen-VL (Bai et al. 2023) was not exposed to medical images during the training of its vision encoder, it lacks the requisite prior knowledge for medical image analysis. Retraining the vision encoder from scratch would be both computationally expensive and logistically complex. To address this limitation, we employ the Pseudo-Augmented Medical Distillation approach, which imparts medical domain knowledge to the model prior to instruction fine-tuning.

Given that the original dataset is formatted in ChatML, which is incompatible with mainstream frameworks, we first reformat it into the ShareGPT format to facilitate processing. In the initial phase of the distillation process, we instantiate two models and fine-tune one of them using 11.1% of the dataset, designating it as the teacher model. Subsequently, leveraging the entire dataset, we perform knowledge distillation into the second model. The distillation loss function is defined as below, ensuring a balanced optimization between standard cross-entropy loss and knowledge distillation loss:

$$\mathcal{L}_{Distill} = \frac{(\mathcal{L}_{CE} + \alpha \mathcal{L}_{KD})}{1 + \alpha} - \frac{\sum_{i=1}^N y_i \log p_s(x_i) + \alpha T^2 \sum_{i=1}^N p_t(x_i) \log \frac{p_t(x_i)}{p_s(x_i)}}{1 + \alpha}$$

Reflective Correction Training

After the model distillation, we restart two rounds of instruction fine-tuning using the complete dataset. During

the instruction fine-tuning process, the model’s outputs are recorded and compared with the ground truth. If the semantic similarity between the output and the ground truth falls below 80%, GPT-4o will correct the output based on the ground truth (retaining only the original meaning and anchor box coordinates) to enrich the diversity of the training set labels. The corrected data is then fed back into the training process for further learning.

Semantic-Aware Selective Generation

The responses generated by large language models exhibit randomness, and relying on a single inference may result in missing the optimal answer. Semantic-Aware Selective Generation means that instead of directly using the model’s single-round generation for evaluation, we allow the model to generate multiple samples. We then utilize the CLIP model to score the alignment between the generated text and image. Finally, we reorder the outputs based on these scores and select the one with the highest score as the final result.

Algorithm 1: Semantic-Aware Selective Generation

- 1: **Input:** Image I , Model M
 - 2: **Output:** Optimal generated text T_{final}
 - 3: $T_1, T_2, \dots, T_n \leftarrow \text{GenerateSamples}(M, I)$
 - 4: **for** $i = 1$ **to** n **do**
 - 5: $S_i \leftarrow \text{CLIPScore}(T_i, I)$
 - 6: **end for**
 - 7: $T_{ordered} \leftarrow \text{Sort}(T_1, T_2, \dots, T_n,)$
 - 8: $T_{final} \leftarrow T_{ordered}[1]$
 - 9: **return** T_{final}
-

Experiments

Datasets

To rigorously validate the effectiveness of our method and training strategy, we conduct training and evaluation on the Med-GRIT-270k dataset. This dataset comprises 270K samples, with 240K allocated for training and the remaining 30K for evaluation. Additionally, we randomly select 30K samples from the entire dataset for pseudo-label generation, which is subsequently used in the distillation process. For further information about the dataset, please refer to the original paper.

Eval Metrics

To ensure a fair comparison with BiRD (Huang et al. 2024), we adopt the same evaluation metrics. Specifically, we use Recall@0.5 for VG, Recall for ROC, SPICE for RC, and mBMR for MIA. The final overall result is computed as the mean of the evaluation scores across these four tasks.

Implementation Details:

We use Qwen2-VL (Wang et al. 2024) as the base model for ClinKD. For the Med-CLIP Guided RoPE component of ClinKD, in order to ensure that the position index is an integer, we resample the image resolution to $w = h$ and set $\gamma_1 = \gamma_2 = 2$. During the distillation process, we set

Model	Test dataset	VG (Recall@0.5 \uparrow)	ROC (Recall \uparrow)	RC (SPICE \uparrow)	MIA (mBMR \uparrow)	Average \uparrow
LLaVa-Med (Li et al. 2023)	Med-GRIT-Test30k	0	2.75	8.18	11.20	5.53
BiRD-Med-GRIT-270k	Med-GRIT-Test30k	53.92	65.33	55.23	52.17	56.66
ClinKD(Ours)	Med-GRIT-Test30k	67.51	82.35	70.56	65.69	71.53
LLaVa-Med (Li et al. 2023)	LLaVa-Med-qa0.2k	-	-	-	20.04	-
BiRD-Med-GRIT-270k	LLaVa-Med-qa0.2k	-	-	-	10.55	-
ClinKD(Ours)	LLaVa-Med-qa0.2k	-	-	-	13.24	-

Table 1: Comparison with LLaVa-Med (Li et al. 2023) and previous SOTA (Huang et al. 2024) and study on the multimodal dataset scales.

Model	VG (Recall@0.5)	ROC (Recall)	RC (SPICE)	MIA (mBMR)	Average
BiRD-Med-GRIT-270k	53.92	65.33	55.23	52.17	56.66
Qwen2-VL-Med-GRIT-270k	55.43 \uparrow	68.33 \uparrow	57.39 \uparrow	62.23 \uparrow	61.37 \uparrow
BiRD+MCG-RoPE	59.73 \uparrow	72.74 \uparrow	61.32 \uparrow	59.63 \uparrow	63.36 \uparrow
BiRD+Pseudo-Lables-KD	63.11 \uparrow	79.52 \uparrow	67.21 \uparrow	64.32 \uparrow	68.54 \uparrow
BiRD+SASG	55.89 \uparrow	67.84 \uparrow	54.32	51.27	57.33 \uparrow
ClinKD(Ours)	67.51\uparrow	82.35\uparrow	70.56\uparrow	65.69\uparrow	71.53\uparrow

Table 2: Ablation study for different models and different strategies(The base model of BiRD is Qwen-VL)

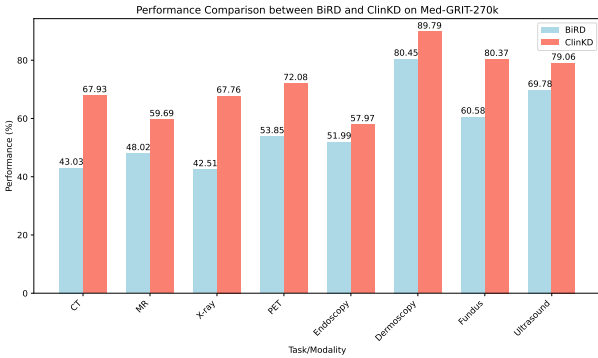


Figure 3: Average scores of 4 tasks arrange different types of data

$\alpha = 0.5$. The number of distillation epochs is 2, with an additional 2 epochs for subsequent training. The entire training process is conducted using 6 NVIDIA A100 40G GPUs. The learning rate is set to 2×10^{-5} , and the AdamW optimizer is employed. The learning scheduler follows a cosine schedule. For model generation, we use non-sampling beam search with a beam size of 3, and for each data point, we generate 3 samples.

Analysis

Comparison with State-of-the-Art Methods Compared to the previously state-of-the-art BiRD, our method achieves superior results without altering the content or quantity of the medical images. As shown in the table, our approach demonstrates significant improvements across four tasks: VG, ROC, RC, and MIA. Specifically, the VG score increased by 13.59%, ROC by 17.02%, RC by 15.33%, and MIA by 13.52%. However, for the LLaVa-Med-qa0.2k

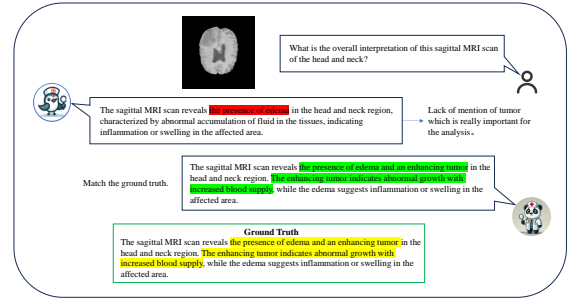


Figure 4: Case study for BiRD and ClinKD

dataset, our results still fall below LLaVA-Med but show an improvement over BiRD. This indicates that our method is still limited in enhancing the model’s generalization ability.

In the BiRD paper, it is suggested that the significant hallucinations generated by the model may be due to the vision encoder not being exposed to a sufficient amount of medical imaging data before being frozen. However, we believe that while the vision encoder greatly impacts the model’s ability to recognize images, the training strategy can help compensate for some of the deficiencies. Our pseudo-label distillation process provides prior knowledge to the model, partially alleviating the lack of medical knowledge in the vision encoder. Subsequently, the Reflective Correction Training enriches the VQA question-answer pairs in the data, thereby improving the utilization of image data. At the model level, Med-CLIP Guided RoPE enhances the model’s ability to perceive different dimensions of image information. These strategies significantly address the shortcomings in the BiRD model and its training approach.

	Metric	CT	MR	X-ray	PET	Endoscopy	Dermoscopy	Fundus	Ultrasound	Average
VG	Recall@0.5 \uparrow	44.47	29.26	41.73	56.46	53.60	75.63	84.15	46.04	53.92
ROC	Recall \uparrow	34.76	61.79	53.74	-	60.40	96.61	-	84.65	65.33
RC	Spice \uparrow	41.88	51.69	37.39	47.95	54.07	77.44	48.73	82.65	55.23
MIA	mBMR \uparrow	47.01	49.35	37.17	57.15	39.91	72.13	48.87	65.78	52.17
Average	-	43.03	48.02	42.51	53.85	51.99	80.45	60.58	69.78	-

Table 3: The performance of the BiRD model across various tasks and modalities on the Med-GRIT-270k test dataset.

	Metric	CT	MR	X-ray	PET	Endoscopy	Dermoscopy	Fundus	Ultrasound	Average
VG	Recall@0.5 \uparrow	65.52	52.23	48.56	69.25	60.37	94.22	86.59	64.47	67.51
ROC	Recall \uparrow	61.42	71.30	97.00	-	68.84	100	-	95.54	82.35
RC	Spice \uparrow	53.94	58.41	71.47	79.91	52.10	83.92	84.51	80.19	70.56
MIA	mBMR \uparrow	66.85	56.82	54.01	67.08	50.58	81.00	70.02	76.05	65.69
Average	-	61.93	59.69	67.76	72.08	57.97	89.79	80.37	79.06	-

Table 4: The performance of the ClinKD model across various tasks and modalities on the Med-GRIT-270k test dataset.

Ablation study Table 2 presents the ablation study of different model architectures and training strategies. First, due to the upgrade of Qwen2-VL, a slight improvement in performance is observed when using the same training approach as BiRD. This enhancement is expected and reasonable. When BiRD incorporates the Med-CLIP Guided RoPE, there is a significant boost in performance on the test set, validating the role of Med-CLIP Guided RoPE in enhancing the model’s modality distinction and image perception.

Similarly, the distilled models, whether Qwen-VL or Qwen2-VL, show substantial improvements in evaluation metrics, which can be attributed to the prior knowledge provided by the pseudo-labels. However, the addition of the SASG module did not result in the anticipated significant performance gain. Instead, it led to only slight fluctuations in the results. We attribute this to the relatively small model parameters, which limit the model’s generative capabilities.

Results Details Figure 3 shows the average scores across four tasks for modalities such as CT, MR, and others, demonstrating significant improvements compared to BiRD.

Tables 3 and 4 present the evaluation details for the eight modalities of BiRD and ClinKD across the four tasks. It is evident that ClinKD outperforms BiRD in most of the evaluations to varying degrees. For instance, MR modality improved by 22.97% on the VG task, indicating that our proposed method alleviates the challenge of generalization caused by the limited anatomical structures of tumor tissues. The CT modality also showed a substantial improvement (26.66%) on the ROC task. Moreover, the Fundus modality exhibited significant improvements in both the RC and MIA tasks, demonstrating that ClinKD is better at distinguishing cross-modal data and performing image-text alignment, thereby enhancing the model’s ability to understand image details and task objectives.

The remaining small fluctuations in scores can be attributed to the inherent randomness in model training distri-

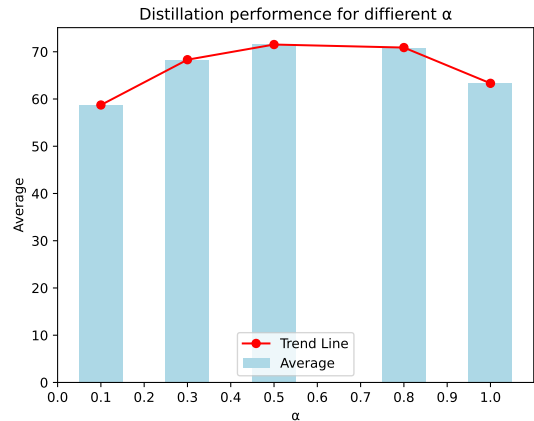


Figure 5: Distillation performance

bution. These issues can be addressed by adjusting the data distribution and distillation ratio.

Overall, the data suggests that ClinKD is more effective in aligning image and text, with superior visual grounding abilities and a stronger understanding of tasks.

Case Study Figure 4 illustrates that both BiRD and ClinKD are capable of analyzing medical images to varying degrees. However, BiRD fails to identify the presence of tumors, instead focusing on describing edematous lesions. This issue stems from the limited MR training data and the direct application of supervised fine-tuning. In contrast, ClinKD benefits from our strategy, which effectively aligns the image-text pairs, allowing its responses to closely match the Ground Truth.

Limitation Although our method alleviates, to some extent, the issue of insufficient prior knowledge and achieves impressive state-of-the-art performance on the Med-GRIT-270k dataset, the model still exhibits hallucinations. Further-

more, through comparative evaluations on the LLaVa-Med-qa0.2k dataset, our approach remains insufficient to enable the model to emerge with strong generalization capabilities in medical question answering. Creating high-quality visual question answering datasets and training medical prior knowledge before freezing the visual encoder could significantly enhance the model’s generalization ability on medical data.

Conclusion

In this paper, we introduce the ClinKD model and a comprehensive set of training strategies. ClinKD employs MedCLIP Guided RoPE to enhance cross-modal discriminative capability and improve the extraction of cross-dimensional image details. Our proposed Pseudo-Augmented Medical Distillation and Reflective Correction Training strategies not only boost data utilization but also provide the model with prior knowledge of medical images to some extent. In terms of generation strategies, SASG steers the model’s responses toward optimal outcomes. These framework components reduce the likelihood of hallucinations, offering a novel approach for enhancing the model’s VQA (Visual Question Answering) and Refer and Grounding capabilities under limited data conditions.

Acknowledgments

This work was supported by the Natural Science Foundation of Guangdong Province (No. 2023A1515010673), in part by the Shenzhen Science and Technology Innovation Bureau key project (No. JSGG20220831110400001, No. CJGJZD20230724093303007, KJZD20240903101259001), in part by Shenzhen Medical Research Fund (No. D2404001), in part by Shenzhen Engineering Laboratory for Diagnosis & Treatment Key Technologies of Interventional Surgical Robots (XMHT20220104009), and the Key Laboratory of Biomedical Imaging Science and System, CAS, for the Research platform support

References

Bai, J.; Bai, S.; Yang, S.; Wang, S.; Tan, S.; Wang, P.; Lin, J.; Zhou, C.; and Zhou, J. 2023. Qwen-VL: A Versatile Vision-Language Model for Understanding, Localization, Text Reading, and Beyond. arXiv:2308.12966.

Hamza, A.; Abdullah; Ahn, Y. H.; Lee, S.; and Kim, S. T. 2024. LLaVA Needs More Knowledge: Retrieval Augmented Natural Language Generation with Knowledge Graph for Explaining Thoracic Pathologies. arXiv:2410.04749.

Huang, X.; Huang, H.; Shen, L.; Yang, Y.; Shang, F.; Liu, J.; and Liu, J. 2024. A Refer-and-Ground Multimodal Large Language Model for Biomedicine. arXiv:2406.18146.

Li, C.; Wong, C.; Zhang, S.; Usuyama, N.; Liu, H.; Yang, J.; Naumann, T.; Poon, H.; and Gao, J. 2023. LLaVA-Med: Training a Large Language-and-Vision Assistant for Biomedicine in One Day. arXiv:2306.00890.

Liu, H.; Li, C.; Wu, Q.; and Lee, Y. J. 2023. Visual Instruction Tuning. arXiv:2304.08485.

Liu, J.; Wang, Y.; Du, J.; Zhou, J. T.; and Liu, Z. 2024. MedCoT: Medical Chain of Thought via Hierarchical Expert. arXiv:2412.13736.

Wang, P.; Bai, S.; Tan, S.; Wang, S.; Fan, Z.; Bai, J.; Chen, K.; Liu, X.; Wang, J.; Ge, W.; Fan, Y.; Dang, K.; Du, M.; Ren, X.; Men, R.; Liu, D.; Zhou, C.; Zhou, J.; and Lin, J. 2024. Qwen2-VL: Enhancing Vision-Language Model’s Perception of the World at Any Resolution. arXiv:2409.12191.

Wei, J.; Wang, X.; Schuurmans, D.; Bosma, M.; Ichter, B.; Xia, F.; Chi, E.; Le, Q.; and Zhou, D. 2023. Chain-of-Thought Prompting Elicits Reasoning in Large Language Models. arXiv:2201.11903.

Zheng, G.; Yang, B.; Tang, J.; Zhou, H.-Y.; and Yang, S. 2023. DDCoT: Duty-Distinct Chain-of-Thought Prompting for Multimodal Reasoning in Language Models. arXiv:2310.16436.